HHS Public Access

Author manuscript

Free Radic Biol Med. Author manuscript; available in PMC 2017 October 24.

Published in final edited form as:

Free Radic Biol Med. 2016 August ; 97: 330–341. doi:10.1016/j.freeradbiomed.2016.06.021.

TRAP-positive osteoclast precursors mediate ROS/NO-dependent bactericidal activity via TLR4

Kazuaki Nishimura[a,b], **Satoru Shindo**[a,c], **Alexandru Movila**[a], **Rayyan Kayal**[d], **Albassam Abdullah**[a,d], **Irma Josefina Savitri**[e], **Atsushi Ikeda**[a], **Tsuguno Yamaguchi**[a,f], **Mohammed Howait**[d], **Ayman Al-dharrab**[d], **Abdulghani Mira**[d], **Xiaozhe Han**[a,g], and **Toshihisa Kawai**[a,g,*]

[a]The Forsyth Institute, Department of Immunology and Infectious Diseases, Cambridge, MA, USA

[b]Tohoku University Hospital, Maxillo-oral Disorders, Sendai, Japan

[c]The University of Tokushima Graduate School, Department of Conservative Dentistry, Institute of Health Biosciences, Tokushima, Japan

[d]King Abdulaziz University, Faculty of Dentistry, Jeddah, Saudi Arabia

[e]Airlangga University, Department of Periodontics, Jawa Timur, Indonesia

[f]Research and Development Headquarters, LION Corporation, 100 Tajima Odawara, Kanagawa, Japan

[g]Harvard School of Dental Medicine, Department of Oral Medicine, Infection and Immunity, Boston, MA, USA

Abstract

Osteoclastogenesis was induced by RANKL stimulation in mouse monocytes to examine the possible bactericidal function of osteoclast precursors (OCp) and mature osteoclasts (OCm) relative to their production of NO and ROS. Tartrate-resistant acid phosphatase (TRAP)-positive OCp, but few or no OCm, phagocytized and killed *Escherichia coli* in association with the production of reactive oxygen species (ROS) and nitric oxide (NO). Phagocytosis of *E. coli* and production of ROS and NO were significantly lower in TRAP+ OCp derived from Toll-like receptor (TLR)-4 KO mice than that derived from wild-type (WT) or TLR_2-KO mice. Interestingly, after phagocytosis, TRAP+ OCp derived from wild-type and TLR2-KO mice did not differentiate into OCm, even with continuous exposure to RANKL. In contrast, *E. coli*-phagocytized TRAP+ OCp from TLR4-KO mice could differentiate into OCm. Importantly, neither NO nor ROS produced by TRAP+ OCp appeared to be engaged in phagocytosis-induced suppression of osteoclastogenesis. These results suggested that TLR4 signaling not only induces ROS and NO production to kill phagocytized bacteria, but also interrupts OCm differentiation. Thus, it can be concluded that TRAP+ OCp, but not OCm, can mediate bactericidal activity via phagocytosis accompanied by the production of ROS and NO via TLR4-associated reprograming toward phagocytic cell type.

*Corresponing author at: Forsyth Institute Department of Immunology and Infectious Diseases, 245 First Street, Cambridge, MA 02142, USA.

Keywords

Osteoclast; Bacteria; Phagocytosis; Toll-like receptor; Tartrate-resistant acid phosphatase; Reactive oxygen species; Nitric oxide; RANKL

1. Introduction

Osteoclast precursors (OCp) are originated from macrophage/monocyte-lineage hematopoietic precursor cells [1,2]. Differentiation from hematopoietic precursor cells to mature osteoclasts (OCm) capable of resorbing bone is elicited by stimulation with receptor activator nuclear factor-κB ligand (RANKL) and macrophage-colony stimulating factor (M-CSF) [3]. Especially, M-CSF plays a key role in the induction of RANK, a receptor for RANKL, on OCp upstream of RANKL-mediated activation of osteoclastogenesis [4]. Indeed, the critical role of M-CSF in the course of osteoclastogenesis was demonstrated by M-CSF-gene knockout (KO) mice that are completely absent of OCm and show osteopetrotic phenotypes [5–8]. It is known that M-CSF-primed monocytes can also differentiate into macrophages in the absence of RANKL and perform antibacterial function [9]. In other words, M-CSF-primed monocytes can differentiate into either macrophages or osteoclasts. Nonetheless, it is largely unknown if monocytes stimulated with both M-CSF and RANKL can mediate antibacterial activity. Both OCp and OCm have been found in infectious bone loss lesion of periodontitis [10–12] and septic prosthesis loosening [13], but it is also largely unknown if OCp and/or OCm can mediate antibacterial activity.

TLR signaling plays a crucial role in the induction of bacterial phagocytosis by macrophages [14]. Activation of TLRs induces macrophages to produce proinflammatory mediators, such as nitric oxide (NO), reactive oxygen species (ROS; e.g., peroxides, superoxide and hydroxyl radical), TNFα and IL-1b [15,16]. Among them, NO and ROS accumulated in phagolysosomes are significantly engaged in bactericidal effects on bacteria phagocytosed by macrophages [17,18]. Interestingly, it is reported that ROS, including superoxide and hydrogen peroxide, are crucial components that upregulate osteoclast differentiation [19–21]. Although the effects of NO on OCp cells are controversial, NO is indeed produced by osteoclasts [22].

In summary, these reported findings have demonstrated 1) the effects of TLRs on NO/ROS production by macrophages that phagocytize bacteria and 2) the engagement of NO/ROS in RANKL-induced osteoclastogenesis. However, it has not been established that TLR signaling can trigger the expressions of NO/ROS and thus facilitate the phagocytosis and killing of bacteria by OCp and/or OCm. Based on these lines of evidence, we hypothesized that TRAP+ OCp, but not OCm, can mediate bactericidal activity via phagocytosis utilizing ROS and NO produced in response to bacteria-derived TLR activation. To test this hypothesis, we performed bacterial phagocytosis assays using OCp and OCm induced from RAW264.7 cells, and primary culture of OCp and OCm derived from bone marrow of TLR2-KO and TLR4-KO as well as their wild type (WT) mice, employing *Escherichia coli* as a model bacterium.

2. Material and methods

2.1. Osteoclastogenesis in vitro

Bone marrow-derived monocyte (BMM) cells were generated as described previously [23,24]. In brief, bone marrow cells isolated from TLR2-KO mice, TLR4-KO mice and their WT (C57BL/6) mice were cultured (1×10^5 cells/well; 96-well plate) in α-modified minimal essential medium (α-MEM) (Life Technologies, Beverly, MA) supplemented with 10% fetal bovine serum (FBS) (Atlanta Biologicals, Lawrenceville, GA). After initial incubation of bone marrow cells with 20 ng/ml M-CSF (BioLegend, San Diego, CA) for 2 days, adherent cells were used as bone marrow-derived monocyte (BMM). Those BMM cells were further stimulated with sRANKL (50 ng/ml) in the presence of M-CSF (20 ng/ml) for various times to induce OCp and OCm. The BMM cells that were incubated in the presence of M-CSF (20 ng/ml) without RANKL for the same periods were used as control macrophages. For the assay using RAW264.7 cells, single cell suspension (2×10^3 cells/well; 96-well plate) in α-MEM with 10% FBS was stimulated with sRANKL (50 ng/ml). Osteoclasts induced in the culture were stained for their expression of TRAP using a commercially available kit (Sigma-Aldrich, St. Louis, MO).

2.2. Bacterial strains and culture

E. coli strain (ATCC27325, Manassas, VA) was cultured overnight at 37 °C in Luria-Bertani (LB) broth medium under constant agitation at 240 rpm. The bacterial number was measured by spectrophotometer at OD 580 nm.

2.3. Assay to determine bacterial phagocytosis and killing by osteo-clasts and macrophages

The method described previously [25–27] was performed with minor changes. In brief, the confluent cells in a 96-well plate with or without RANKL were cultured in antibiotic-free medium overnight prior to the bacterial phagocytosis assay. Live bacteria harvested at mid-log growth curve were co-cultured with the cells for 1 h in antibiotic-free medium at an MOI of 10. After 1 h of co-culture, extracellular bacteria that did not enter cells were killed by treatment with gentamicin (500 μg/ml; Life Technologies) applied over the course of 1 h. After additional incubation for 1 h, 2 h and 3 h, live bacteria remaining inside cells were released by osmotic shock-dependent disruption using distilled water (100 ml/well), followed by extensive pipetting (20 strokes/well). Bacterial suspension was spread to LB agar (Sigma-Aldrich) plates, and the number of colonies was counted. The Colony Forming Unit (CFU) corresponds to the number of colonies observed in an agar plate. The CFU was further normalized based on the OCps present in the well, and expressed as CFU/1000 OCps. The protocol used for this assay is illustrated in Fig. 1A.

In some experiments, after the antibiotics treatment, BMM cells or RAW264.7 cells were cultured in fresh medium in the presence or absence of NAC (1 mM), L-NAME (1 mM) or D-NAME (1 mM). Subsequently, the CFU of survived *E. coli* was also monitored, while the culture supernatant was subject to the measurements of NO_2^- and TOS (see below).

2.4. Flow cytometry analysis of pHrodo™ uptake by RAWS264.7 cells and BMM cells

Phagocytosis of bacteria by osteoclasts and macrophages was also evaluated using flow cytometry. This was performed using pHrodo™ BioParticles® [28]. Phagocytized pHrodo-labeled *E. coli* fluoresced in an acidic pH-dependent manner. Briefly, pHrodo (fixed *E. coli*) was incubated with live RAW264.7 cells or BMM cells for 1 h at 37 °C. Cells incubated with pHrodo on ice were used as negative control. Cells were harvested by Falcon™ cell scraper (Thermo Fisher), washed three times, and then subjected to flow cytometry or confocal fluorescent microscopy. Data were analyzed using FlowJo software (Treestar, Ashland, OR).

2.5. Determination of nitrite (NO_2^-) concentrations

The levels of nitric oxide (NO) in the macrophage/osteoclast medium were measured by Griess assay [29,30]. Briefly, 50 μL of culture supernatants were gently mixed with an equal volume of 2% sulfanilamide (Sigma) solution and incubated in the dark at room temperature for 10 min. After incubation, 50 μL of naphthyl etilenediamine dihydrochloride (Sigma) in 5% phosphoric acid solution were added to the reaction and incubated in the dark at room temperature for another 10 min. The absorbance at 540 nm was measured in a microplate reader. Nitrite concentration, an indicator of NO production, was calculated from a $NaNO_2$ standard curve.

2.6. Total oxidant status (TOS) assay

TOS in cells was measured following the method previously reported by Erel [31]. The oxidants in the sample oxidize the ferrous ion-o-dianisidine complex to ferric ion. The ferric ion produced a colored complex with xylenol orange in an acidic medium. The color intensity, as measured spectrophotometrically, was related to the total amount of oxidant molecules present in the sample. The assay was calibrated with hydrogen peroxide (H_2O_2), and the results were expressed in terms of micromolar hydrogen peroxide equivalent per liter (μmol H_2O_2 equivalent/L).

2.7. Immunofluorescence microscopy

Macrophages and osteoclasts imaged with confocal microscopy were plated on eight-well chamber slides (Lab-Tek Chamber Slide, Thermo Fisher). Images were acquired on a confocal microscope (Zeiss LSM780, Carl Zeiss Microscope, Thornwood, NY). To observe phagocytized pHrodo™ *E. coli* BioParticles®, cells were fixed in 4% paraformaldehyde for 30 min and stained with Alexa Fluor® 488-conjugated phalloidin (Life Technologies) and counterstained with DAPI (Life Technologies).

2.8. Statistical analysis

All assays were conducted at least in triplicate, and each study was repeated 3 times. The collected data were analyzed using the Student's *t*-test for the comparison between two groups, or a one-way ANOVA with post hoc Tukey's test for the comparisons among different groups. *P* values of <0.05 were considered statistically significant.

3. Results

3.1. RANKL-stimulated osteoclasts can phagocytize bacteria

In order to examine if RANKL-stimulated osteoclast precursors (OCp) and/or mature osteoclasts (OCm) could phagocytize bacteria, *E. coli* was incubated with RANKL-stimulated or non-stimulated RAW264.7 cells for various times (Fig. 1). More specifically, RAW264.7 cells were preincubated with or without RANKL for 2 days or 4 days prior to the addition of *E. coli*. The phagocytized bacterial number (CFU/1000 mononuclear cells) by the cytoplasm of RAW264.7 cells detected at baseline (0 h) was higher in nonstimulated RAW264.7 cells than that in the cytoplasm of RAW264.7 cells prestimulated with RANKL for 48 h (non-stimulated, 159±65 CFU/1000 mononuclear cells; RANKL-prestimulated, 43±7 CFU/1000 mononuclear cells; $p<0.01$) (Fig. 1B and C). Even with RANKL stimulation for 96 h, the bacteria phagocytized by RAW264.7 cells at baseline (0 h) showed no significant difference from those phagocytized by RAW264.7 cells prestimulated with RANKL for 48 h (Fig. 1D and E). According to TRAP staining (Fig. 1F), all RAW264.7 cells were TRAP-positive after stimulation with RANKL for more than 48 h, while the number of multinuclear OCm significantly increased in those RAW264.7 cells prestimulated with RANKL for 96 h (TRAP multinuclear OCm cell number: 48 h, 15±7 cells/well; 96 +h, 256±65 cells/well; data not shown in Fig. 1). Both nonstimulated and RANKL-prestimulated RAW264.7 cells appeared to kill phagocytized bacteria in a time-dependent fashion. Such observations were more evident when the % of killing effects was calculated (Fig. 1G and H). RAW264.7 cells were prestimulated with RANKL for 2 days and 4 days, and after 3 h of incubation with *E. coli* at each time point, 62.1±1.0% and 50.8±4.9% of bacteria were killed, respectively ($p<0.01$), suggesting that osteoclast differentiation impairs bactericidal effects by RANKL-prestimulated RAW264.7 cells. No statistical difference was observed in bactericidal effects by unstimulated RAW264.7 cells cultured in medium alone for 2 and 4 days (Fig. 1G and H).

3.2. Mononuclear, but not multinuclear, osteoclasts can phagocytize bacteria

Fixed *E. coli* labeled with a pH-sensitive fluorescent dye (pHrodo) was used to examine the phagocytosis of bacteria by RANKL-stimulated mononuclear and multinuclear cells. Upon phagocytization of pHrodo-labeled *E. coli* in the acidic environment of host cell cytoplasm, red fluorescence is emitted. After incubation of RAW264.7 cells with pHrodo-labeled *E. coli*, the number of bacteria positive for red pHrodo was counted under the fluorescent microscope (Fig. 2A, B and C). After 1 h incubation with bacteria, 91.7±3.2% of unstimulated RAW264.7 cells showed bacterial entry into cytoplasm. In contrast, 28.8±5.2% of RANKL-prestimulated RAW264.7 mononuclear cells showed cytoplasmic entry of pHrodo-labeled *E. coli*. On the other hand, only 2.3±0.4% multinuclear cells showed phagocytosis of pHrodo-labeled *E. coli* ($p<0.01$) (Fig. 2F). It is important to note that all RANKL-prestimulated RAW264.7 cells were TRAP-positive, whereas non-stimulated RAW264.7 cells showed no TRAP staining pattern in separately prepared culture (Fig. 2D and E). To summarize, nearly 80% of non-stimulated RAW264.7 cells showed cytoplasmic entry of pHrodo-labeled *E. coli*, whereas about 30% of RANKL-prestimulated mononuclear, but not multinuclear, RAW264.7 cells internalized pHrodo-labeled *E. coli*. Therefore, these results support the phagocytosis of *E. coli* by mononuclear OCp. According to flow

cytometry, the mononuclear cell population in RANKL-prestimulated RAW264.7 cells showed a smaller percentage (49.9%) of pHrodo-positive cells compared to unstimulated RAW264.7 cells (75.6%), corresponding to the results obtained using fluorescent microscopy.

3.3. Osteoclasts produce ROS and NO in response to bacterial stimulation

Since the production of NO and ROS is significantly promoted in macrophage phagocytosis [17,18], we hypothesized that NO and ROS produced by RANKL-stimulated RAW264.7 cells could kill the phagocytized bacteria. To test this idea, RAW264.7 cells, both unstimulated and prestimulated with RANKL for 48 h and 96 h, incubated with *E. coli* induced a significantly elevated production of ROS (Fig. 3A) and NO (Fig. 3D). However, no temporal difference was noted in the production of either NO or ROS from RAW264.7 cells in response to *E. coli* stimulation after two or four days of preincubation with or without RANKL, suggesting that similar levels of NO and ROS are produced by OCp at early stage (48 h) and mid-stage (96 h) of differentiation. The addition of N-acetyl-L-cysteine (NAC), an ROS inhibitor, or NG-nitro-L-arginine methyl ester (L-NAME), an NO inhibitor, but not the addition of control NG-nitro-D-arginine methyl ester (D-NAME), significantly suppressed the *E. coli*-induced production of ROS or NO in RAW264.7 cells prestimulated with or without RANKL for 48 h (Fig. 3B and C, ROS production; E and F, NO production) and 96 h (not shown). The possible bactericidal roles of ROS and NO on *E. coli* phagocytized by RANKL-stimulated OC were further evaluated in the following experiments using primary culture of OCp isolated from mouse bone marrow (Fig. 6).

3.4. TLR4 is engaged in the induction of bacterial phagocytosis

To investigate whether TLRs are involved in phagocytosis of RANKL-stimulated monocytes (OCp and/or OCm), bone marrow-derived monocytes (BMM) isolated from WT, TLR2-KO and TLR4-KO mice were used (Fig. 4A–E). BMM isolated from different strains of mice were stimulated with M-CSF and RANKL to induce osteoclastogenesis, while M-CSF alone without RANKL was used for control macrophages. Nearly all M-CSF/RANKL-stimulated BMM cells (94–98%) were TRAP-positive (Fig. 4A). There were no remarkable difference in the morphology (Fig. 4A) OCps and OCms differentiated from TLR2-KO and TLR4-KO mice compared to their WT mice. The number of TRAP+ OCms also did not show any significant difference among those three groups (Supplement Fig. 1). After prestimulation with M-CSF and RANKL, or M-CSF alone, for 48 h or 96 h, pHrodo-labeled *E. coli* was applied to the respective cell culture. The incidence of pHrodo-positive red fluorescence, indicating phagocytized *E. coli* in unstimulated TLR4-KO BMM cells (75.7±4.5%), was significantly lower than that in WT (89.6±2.9%) ($p<0.05$) or TLR2-KO mice (90.0±5.6%) ($p<0.05$) (Fig. 4B and D). The incidence of pHrodo-positive RANKL-stimulated TLR4-KO BMM cells (mononuclear OCp, 30.0%±3.0%; multinuclear OCm, 1.3±2.4%) was lower than that in WT (mononuclear OCp, 62.8±4.7%, $p<0.01$; multinuclear OCm, 9.4±2.2%, $p<0.05$) or TLR2-KO mice (mononuclear OCp, 63.1±2.8%, $p<0.01$; multinuclear OCm, 9.4%±1.2%, $p<0.05$) (Fig. 4B and E). On the other hand, no significant difference was observed in the incidence of pHrodo-positive cells between WT and TLR2-KO BMM cells (Fig. 4B, C and D). According to flow cytometry analysis (Fig. 4E), the mononuclear cell population (OCp) of RANKL-prestimulated TLR4-KO BMM showed a significantly lower level of

phagocytization of pHrodo-positive *E. coli* than either WT or TLR2-KO mice, corresponding to the results from fluorescent microscopy.

In order to examine the possible engagement of TLR2 and/or TLR4 in the production of ROS and NO from primary culture of OCp in response to the exposure with *E. coli*, the production of *E. coli*-induced ROS (Fig. 5A and C) and NO (Fig. 5B and D) from M-CSF+ RANKL-prestimulated OCp was examined using BMM cells derived from WT, TRL2-KO and TLR4-KO mice. Similar to the results from RAW264.7 cells (Fig. 3), the OCp induced from BMM by prestimulation with M-CSF+RANKL for 48 h showed significantly elevated production of ROS (Fig. 5A) and NO (Fig. 5B) in response to *E. coli* exposure. In terms of OCp cells derived from BMM cells prestimulated with M-CSF+RANKL for 48 h (Fig. 5C), ROS production from TLR4-KO OCp cells (13.2±2.1 μmol H_2O_2 equivalent/L), but not TLR2-KO OCp cells (15.1±0.9 μmol H_2O_2 equivalent/L), was significantly lower level than that of WT OCp cells (16.8±1.16 μmol H_2O_2 equivalent/L) ($p<0.05$) in the group prestimulated with M-CSF and RANKL for 48 h (Fig. 5C). OCp cells derived from BMM cells prestimulated with M-CSF + RANKL for 96 h showed the same trend of significantly diminished *E. coli-induced* ROS production by TLR4-KO BMM cells, compared to that (data not shown). The amount of *E. coli*-induced NO production from TLR2-KO OCp cells (1.7±0.1 [NO_2^-] μmol/l) and TLR4-KO OCp cells (1.4±0.1 [NO_2^-] μmol/l) was significantly lower than that detected from WT OCp cells (2.4±0.3 [NO_2^-] μmol/l) ($p<0.01$) in the group of OCp derived from BMM prestimulated with M-SCF and RANKL for 48 h (Fig. 5D). The group prestimulated with M-CSF+RANKL for 96 h demonstrated results of *E. coli*-induced NO production similar to those found in the 48 h MSCF+RANKL prestimulation group (data not shown). The production of ROS and NO from *E. coli*-exposed OCp derived from WT, TLR2-KO and TLR4-KO mice was suppressed in all cases by the addition of NAC, as well as L-NAME to the base line level (Fig. 5C and D). We did not find any difference in the susceptibility to NAC and L-NAME-mediated ROS and NO suppression among the three strains of mice for their production.

The bactericidal effects on phagocytized bacteria were also observed in the primary culture of BMM-derived OCp (Fig. 6). Bacteria killing rate of control BMM preincubated with M-CSF alone showed no difference among WT, TLR2-KO and TLR4-KO mice (Fig. 6A). However, the bacteria killing rate by TLR4-KO OCp was significantly lower that of WT or TLR2-KO mice (Fig. 6B). Furthermore, NAC and L-NAME downregulated bactericidal effects on phagocytized bacteria in OCp (Fig. 6B) as well as control M-CSF-prestimulated BMM (macrophages, Fig. 6A), suggesting that OCp killed the phagocytized bacteria in an ROS/NO-dependent manner, similar to macrophages. Interestingly, the bacteria killing effects by OCp derived from TLR4-KO mice were suppressed significantly more by NAC and L-NAME than that detected in WT or TLR2-KO. These results indicated that ROS and NO produced by OCp via TLR4-activation are in part associated with the bacteria killing effects on the phagocytized bacteria.

3.5. Bacterial phagocytosis inhibits OCp from RANKL-dependent osteoclast maturation in a manner independent of ROS and NO productions

Finally, since ROS and NO are known to promote the RANKL-mediated osteoclastogenesis [19,20,32], we asked if phagocytizing OCp which increase production of ROS and NO could affect their RANKL-mediated differentiate into OCm. To examine this, osteoclast precursors developed in vitro from BMM of WT, TLR2-KO and TLR4-KO mice were exposed to *E. coli* and, subsequently, maintained in culture under continuous RANKL stimulation. More specifically, after prestimulation of BMM cells with M-CSF and RANKL for 48 h, these OCp cells were incubated with or without fixed *E. coli* for 3 h, followed by continuous incubation with RANKL for an additional 5 days. In the absence of bacterial exposure, all OCp isolated from WT, TLR2-KO and TLR4-KO mice differentiated into TRAP+ multinucleated OCm at comparable levels (Fig. 7H). On the other hand, contrary to our expectation, exposure to *E. coli* nearly completely inhibited the differentiation of OCp derived from WT and TLR2-KO mice (Fig. 7B and H). However, the OCp derived from TLR4-KO mice did differentiate into TRAP+ multinucleated OCm, albeit osteoclast size was smaller (Fig. 7E and H) than that found in osteoclasts differentiated in the absence of *E. coli* (Fig. 7C, D and H). Incubation of OCp cells with LPS (TLR4 ligand) and lipoteichoic acid (LTA; TLR2 ligand) suppressed RANKL-induced osteoclastogenesis (Fig. 7I). Importantly, at least 100-fold higher amount of LTA than LPS was required to completely suppress osteoclast differentiation (Fig. 7F, G and I), indicating that TLR4 activation has a greater magnitude of impact on osteoclastogenesis than that by TLR2 activation. These results implicated that bacterial exposure to OCp inhibits their differentiation into OCm, in part from the signal elicited by TLR4 activation. Finally, we examined the core question as to whether ROS or NO is engaged in the altered osteoclastogenesis in bacteria phagocytizing OCp (Fig. 7J). When either NAC or L-NAME was added to the culture of *E. coli*-phagocytizing WT OCp which were continuously incubated with RANKL, neither one abrogated the suppression of osteoclastogenesis resulting from exposure to *E. coli* (Fig. 7J), suggesting that neither ROS nor NO is engaged in *E. coli*-mediated suppression of osteoclastogenesis.

4. Discussion

The present study demonstrated that mononuclear osteoclast precursor cells (OCp), but not mature multinucleated osteoclasts (OCm), can phagocytize *E. coli* and kill phagocytized *E. coli* in association with the production of reactive oxygen species (ROS) and nitric oxide (NO). Both phagocytosis of *E. coli* and ROS and NO production were significantly lower in OCp derived from TLR4-KO mice than compared to wild-type (WT) and TLR2-KO mice. Furthermore, the OCp of wild-type and TLR2-KO mice that did phagocytize *E. coli* did not differentiate into OCm, even with continuous exposure to RANKL, whereas *E. coli*-phagocytized OCp of TLR4-KO mice could differentiate into OCm. The addition of NAC (ROS inhibitor) and L-NAME (NO inhibitor) did not abrogate the diminished differentiation of *E. coli*-phagocytized OCp to OCm by continuous exposure to RANKL, suggesting that neither ROS nor NO is associated with such bacterial phagocytosis-related interruption of OCp differentiation. These results clearly demonstrated that TLR4 signaling not only induces ROS and NO production to kill phagocytized bacteria, but also downregulates

differentiation toward OCm. Osteoclasts have always been considered bone-resorbing cells; therefore, the findings in this study may gain new insight into the etiology of osteoimmunological disorders where monocytes differentiate into osteoclast precursors.

Along with neutrophils, macrophages play a key role in innate immune responses toward bacterial infection based on their function to phagocytize and kill bacteria. Antibacterial activities by macrophages are, in part, mediated by their production of free radicals, including nitric oxide (NO) and reactive oxygen species (ROS) [18]. Bacteria phagocytized by macrophages are destroyed in the phagolysosome via oxygen-dependent and oxygen-independent mechanisms. As an oxygen-dependent bacteria-killing mechanism, free radicals, such as ROS and NO, are generated, while digestive enzymes, for example, lysozyme and cathepsin, are also utilized in the bacteria-killing mechanism [33,34]. Furthermore, lines of evince support ROS and NO as cell signaling molecules in innate immune cells [35,36]. Interestingly, ROS produced by osteoclasts play a role in promoting the differentiation of these cells through Akt, NF-κB and ERK activation [37,38], suggesting that ROS function as a cell signaling mediator in osteoclastogenesis. Recent study reported that ROS-induced promotion of osteoclastogenesis is downmodulated by an antioxidant response system involving Nerf2 in the homeostatic context [39,40], indicating the presence of a sophisticated regulatory mechanism for ROS-associated osteoclastogenesis. On the other hand, low level of NO increases the generation of mature osteoclasts by up-regulating actin remodeling in mononuclear preosteoclasts, thereby promoting cell fusion processes required for multi-nucleation of OCm [32]. In contrast, high concentration of NO inhibits osteoclastogenesis and activity of OCm, while same high level of NO induces apoptosis in OCp [41]. In sum, the effects NO on osteoclastogenesis are dependent on the concentration of NO released in the microenvironment surrounding OCp or OCm. Surprisingly, antibacterial roles of NO and ROS produced by osteoclasts have not been addressed until the present study. Our results demonstrated that ROS and NO produced by OCp are engaged in bactericidal effects. The chemical inhibitors that interrupt the generation of ROS and NO, i.e., NAC and L-NAME, respectively, suppressed their bactericidal effects on phagocytized bacteria in OCp (Fig. 6). The concentration of NAC and L-NAME that showed nearly complete suppression of ROS and NO production by osteoclasts (Fig. 3 and 5) could downregulate the bactericidal effects at the rate of 35–45% (Fig. 6), suggesting that other factors, such as lysozyme or cathepsin, are involved in bactericidal effects by OCp in addition to ROS and NO.

The activation of macrophages through Toll-like receptor (TLR) signaling pathways consists of a major component in the innate immune responses to bacterial infection [42]. Activation of Toll-like receptors, such as TLR1, TLR2 and TLR4, results in the generation of ROS and NO from macrophages by means of nicotinamide adenine dinucleotide phosphate (NADPH) oxidases, myeloperoxidase, mitochondria, or NO-producing enzymes [43]. However, as noted above, while ROS and NO produced by osteoclasts are known to be engaged in osteoclast differentiation [32,37,38], the role of TLRs in the induction of ROS and NO has been elusive. On the other hand, the impact of TLR activation on osteoclastogenesis appears to be more complex than that on macrophages. That is, TLR signals inhibit RANKL-induced osteoclast differentiation in the early precursor stage, whereas differentiation of mid-late stage of RANKL-primed osteoclasts is promoted by TLR signaling [44,45]. Our results

demonstrated that RANKL-stimulated mononuclear TRAP+ OCp can kill bacteria in manner similar to that of macrophages, in which activation of TLR4, but little or no activation of TLR2, is involved the induction of phagocytosis (Fig. 4) and ROS/NO production (Fig. 6). However, this same TLR4 signaling appeared to be engaged in the suppression of osteoclastogenesis in TRAP+ OCp cells challenged with *E. coli* in a manner independent of NO/ROS produced by stimulation with *E. coli* (Fig. 7). More specifically, *E. coli*-mediated suppression of osteoclastogenesis was partially abrogated in the TRAP+ OCp derived from TLR4-KO mice in response to continuous exposure to RANKL, whereas *E. coli* completely suppressed osteoclastogenesis in TRAP+ OCp derived from TLR2-KO or WT mice that were also continuously exposed to RANKL. That TLR4 is partially involved in *E. coli*-induced suppression of osteoclastogenesis seems incongruent with its promotion of RANKL-induced osteoclastogenesis by induction of ROS and NO production. This discrepancy indicates the presence of some unknown signaling pathway elicited by TLR4 which does not involve ROS/NO downregulation of osteoclastogenesis.

One of the key findings in this study is that phagocytosis of *E. coli* was observed in OCps, but not in OCms. According to our unpublished result, similar to *E. coli*, phagocytosis of Gram (+) bacterium, *Enterococcus faecalis* (*Ef*), was also found in OCps, but not in OCms (data not shown). However, as fluorescent micro-particle (fluorescent latex beads ø=0.75 μm) was applied to the osteoclast phagocytosis assay, both OCps and OCms phagocytized fluorescent micro-particle (data not shown). In correspond to the latter finding, latex and PMMA particles were reported to be phagocytized by OCms [46]. Meng et al. also reported that OCms can phagocytize titanium particle (ø<1 mm) and that the expressions of osteoclast-maturation genes, including, TRAP and cathepsin K, were inhibited by a higher concentration of titanium particles, but enhanced at a lower concentration of titanium particles [47]. Since the sizes of fluorescent micro-particle and titanium are similar to that of *E. faecalis* (ø=0.6–2.0 mm, cocci) and *E. coli* (0.5 × 2 μm, rod), it appeared that molecules distinctly expressed on bacteria regulate selective phagocytosise by OCps. As noted above, at least, TLRs are engaged in the induction of phagocytosis of bacteria by OCps.

The addition of LTA, a TLR2 ligand, to TRAP+ OCp suppressed osteoclastogenesis to a lesser degree compared to LPS, a TLR4 ligand (Fig. 7), suggesting that TLR ligand(s) other than those of TLR4 are present on bacteria phagocytized by OCp and may also contribute to the suppression of osteoclastogenesis. Interestingly, it was demonstrated that *Ef* suppress the differentiation of macrophages into osteoclasts [48], and that activation of TLR2 by LTA produced by *Ef* is in part engaged in the attenuation of osteoclastogenesis [49]. Indeed, various TLR ligands inhibit RANKL-mediated osteoclastogenesis from OCp [50–52]. One of the theories underlying TLR-elicited inhibition of osteoclastogenesis is the autocrine production of IFN-β [53,54] which, in turn, suppresses the expression of c-Fos protein, a pivotal transcription factor for the formation of osteoclasts [55]. The latter studies were carried out using mouse OCp. However, in terms of human OCp, it is reported that TLR ligands suppress osteoclastogenesis by inhibiting expression of receptor activator of NF-κB (RANK), thereby making precursor cells refractory to the effects of RANKL [56]. The detailed molecular mechanism underlying the suppression of RANKL-induced osteoclastogenesis caused by phagocytized bacteria in OCp will be addressed in future studies.

Our current working hypothesis supports that phagocytic property by OCps may play a role in prevention of the bacterial dissemination into the bone in the context of infectious bone lytic disease, such as periodontitis. Especially it has become evident that OCps in the circulation migrate to intact bone as well as inflammatory bone resorption lesion and participate in bone resorption [57,58], suggesting that OCps function similar to innate immune macrophages [59]. For this reason, it is plausible that any pharmaceutical intervention for bone lytic diseases that targets osteoclast differentiation, such as bisphosphonate and Denosumab [60,61], would attenuate the OCps-mediated anti-bacterial barrier mechanism for alveolar bone. As a consequence of attenuated antibacterial function by OCps which permits the invasion of bacteria into bone, osteonecrosis of jaw may be induced [62].

In conclusion, the present study showed that RANKL-stimulated, TRAP-positive OCp can phagocytize and then kill bacteria through TLR4 signaling and induction of ROS/NO, respectively.

Supplementary Material

Refer to Web version on PubMed Central for supplementary material.

Acknowledgments

This work was partially supported by NIH grants RO1 DE-018499, RO1 DE-019917, R56 DE023807 and R01DE025255 and T32 DE 7327-12 from National Institute of Dental and Craniofacial Research (NIDCR) and a research fund from King Abdulaziz University (KAU).

Appendix A. Supplementary material

Supplementary data associated with this article can be found in the online version at http://dx.doi.org/10.1016/j.freeradbiomed.2016.06.021.

References

1. Teitelbaum SL, Ross FP. Genetic regulation of osteoclast development and function. Nat Rev Genet. 2003; 4(8):638–649. [PubMed: 12897775]
2. Xing L, Schwarz EM, Boyce BF. Osteoclast precursors, RANKL/RANK, and immunology. Immunol Rev. 2005; 208:19–29. [PubMed: 16313338]
3. Asagiri M, Takayanagi H. The molecular understanding of osteoclast differentiation. Bone. 2007; 40(2):251–264. [PubMed: 17098490]
4. Suda T, Takahashi N, Udagawa N, Jimi E, Gillespie MT, Martin TJ. Modulation of osteoclast differentiation and function by the new members of the tumor necrosis factor receptor and ligand families. Endocr Rev. 1999; 20(3):345–357. [PubMed: 10368775]
5. Hattersley G, Owens J, Flanagan AM, Chambers TJ. Macrophage colony stimulating factor (M-CSF) is essential for osteoclast formation in vitro. Biochem Biophys Res Commun. 1991; 177(1): 526–531. [PubMed: 2043138]
6. Tanaka S, Takahashi N, Udagawa N, Tamura T, Akatsu T, Stanley ER, Kurokawa T, Suda T. Macrophage colony-stimulating factor is indispensable for both proliferation and differentiation of osteoclast progenitors. J Clin Investig. 1993; 91(1):257–263. [PubMed: 8423223]
7. Yoshida H, Hayashi S, Kunisada T, Ogawa M, Nishikawa S, Okamura H, Sudo T, Shultz LD, Nishikawa S. The murine mutation osteopetrosis is in the coding region of the macrophage colony stimulating factor gene. Nature. 1990; 345(6274):442–444. [PubMed: 2188141]

8. Wiktor-Jedrzejczak W, Bartocci A, Ferrante AW Jr, Ahmed-Ansari A, Sell KW, Pollard JW, Stanley ER. Total absence of colony-stimulating factor 1 in the macrophage-deficient osteopetrotic (op/op) mouse. Proc Natl Acad Sci USA. 1990; 87(12):4828–4832. [PubMed: 2191302]

9. Stanley ER, Berg KL, Einstein DB, Lee PS, Yeung YG. The biology and action of colony stimulating factor-1. Stem Cells. 1994; 12(Suppl. 1):S15–S24. (discussion 25).

10. Carson RE, Sayegh FS, Fedi PF Jr. Osteoclastic resorption of alveolar bone affected by periodontitis–correlation of light microscopic and scanning electron microscopic observations. J Periodontol. 1978; 49(8):406–414. [PubMed: 112239]

11. Okada H, Kida T, Yamagami H. Identification and distribution of immunocompetent cells in inflamed gingiva of human chronic periodontitis. Infect Immun. 1983; 41(1):365–374. [PubMed: 6602770]

12. Thorbert-Mros S, Larsson L, Berglundh T. Cellular composition of long-standing gingivitis and periodontitis lesions. J Periodontal Res. 2015; 50(4):535–543. [PubMed: 25330403]

13. Gehrke T, Sers C, Morawietz L, Fernahl G, Neidel J, Frommelt L, Krenn V. Receptor activator of nuclear factor kappaB ligand is expressed in resident and inflammatory cells in aseptic and septic prosthesis loosening. Scand J Rheumatol. 2003; 32(5):287–294. [PubMed: 14690142]

14. Medzhitov R. Toll-like receptors and innate immunity. Nat Rev Immunol. 2001; 1(2):135–145. [PubMed: 11905821]

15. Janeway CA Jr, Medzhitov R. Innate immune recognition. Annu Rev Immunol. 2002; 20:197–216. [PubMed: 11861602]

16. West AP, Brodsky IE, Rahner C, Woo DK, Erdjument-Bromage H, Tempst P, Walsh MC, Choi Y, Shadel GS, Ghosh S. TLR signalling augments macrophage bactericidal activity through mitochondrial ROS. Nature. 2011; 472(7344):476–480. [PubMed: 21525932]

17. Prolo C, Alvarez MN, Radi R. Peroxynitrite, a potent macrophage-derived oxidizing cytotoxin to combat invading pathogens. BioFactors. 2014; 40(2):215–225. [PubMed: 24281946]

18. Weiss G, Schaible UE. Macrophage defense mechanisms against intracellular bacteria. Immunol Rev. 2015; 264(1):182–203. [PubMed: 25703560]

19. Garrett IR, Boyce BF, Oreffo RO, Bonewald L, Poser J, Mundy GR. Oxygen-derived free radicals stimulate osteoclastic bone resorption in rodent bone in vitro and in vivo. J Clin Investig. 1990; 85(3):632–639. [PubMed: 2312718]

20. Key LL Jr, Ries WL, Taylor RG, Hays BD, Pitzer BL. Oxygen derived free radicals in osteoclasts: the specificity and location of the nitroblue tetrazolium reaction. Bone. 1990; 11(2):115–119. [PubMed: 2162696]

21. Kim H, Kim IY, Lee SY, Jeong D. Bimodal actions of reactive oxygen species in the differentiation and bone-resorbing functions of osteoclasts. FEBS Lett. 2006; 580(24):5661–5665. [PubMed: 16996506]

22. Wimalawansa SJ. Rationale for using nitric oxide donor therapy for prevention of bone loss and treatment of osteoporosis in humans. Ann N Y Acad Sci. 2007; 1117:283–297. [PubMed: 18056048]

23. Lee NK, Choi YG, Baik JY, Han SY, Jeong DW, Bae YS, Kim N, Lee SY. A crucial role for reactive oxygen species in RANKL-induced osteoclast differentiation. Blood. 2005; 106(3):852–859. [PubMed: 15817678]

24. Franco GC, Kajiya M, Nakanishi T, Ohta K, Rosalen PL, Groppo FC, Ernst CW, Boyesen JL, Bartlett JD, Stashenko P, Taubman MA, Kawai T. Inhibition of matrix metalloproteinase-9 activity by doxycycline ameliorates RANK ligand-induced osteoclast differentiation in vitro and in vivo. Exp Cell Res. 2011; 317(10):1454–1464. [PubMed: 21420951]

25. Kajiya M, Komatsuzawa H, Papantonakis A, Seki M, Makihira S, Ouhara K, Kusumoto Y, Murakami S, Taubman MA, Kawai T. Aggregatibacter actinomycetemcomitans Omp29 is associated with bacterial entry to gingival epithelial cells by F-actin rearrangement. PLoS One. 2011; 6(4):e18287. [PubMed: 21559515]

26. Lawrence DW, Kornbluth J. E3 ubiquitin ligase NKLAM is a macrophage phagosome protein and plays a role in bacterial killing. Cell Immunol. 2012; 279(1):46–52. [PubMed: 23085241]

27. McEachern EK, Hwang JH, Sladewski KM, Nicatia S, Dewitz C, Mathew DP, Nizet V, Crotty Alexander LE. Analysis of the effects of cigarette smoke on staphylococcal virulence phenotypes. Infect Immun. 2015; 83(6):2443–2452. [PubMed: 25824841]

28. Matsui A, Jin JO, Johnston CD, Yamazaki H, Houri-Haddad Y, Rittling SR. Pathogenic bacterial species associated with endodontic infection evade innate immune control by disabling neutrophils. Infect Immun. 2014; 82(10):4068–4079. [PubMed: 25024367]

29. Green LC, Wagner DA, Glogowski J, Skipper PL, Wishnok JS, Tannenbaum SR. Analysis of nitrate, nitrite, and [15N]nitrate in biological fluids. Anal Biochem. 1982; 126(1):131–138. [PubMed: 7181105]

30. Tsutsuki H, Yahiro K, Suzuki K, Suto A, Ogura K, Nagasawa S, Ihara H, Shimizu T, Nakajima H, Moss J, Noda M. Subtilase cytotoxin enhances Escherichia coli survival in macrophages by suppression of nitric oxide production through the inhibition of NF-kappaB activation. Infect Immun. 2012; 80(11):3939–3951. [PubMed: 22949549]

31. Erel O. A new automated colorimetric method for measuring total oxidant status. Clin Biochem. 2005; 38(12):1103–1111. [PubMed: 16214125]

32. Nilforoushan D, Gramoun A, Glogauer M, Manolson MF. Nitric oxide enhances osteoclastogenesis possibly by mediating cell fusion. Nitric Oxide: Biol Chem. 2009; 21(1):27–36.

33. Elsbach P, Weiss J. Oxygen-dependent and oxygen-independent mechanisms of microbicidal activity of neutrophils. Immunol Lett. 1985; 11(3–4):159–163. [PubMed: 3910565]

34. Elsbach P, Weiss J. A reevaluation of the roles of the O2-dependent and O2-independent microbicidal systems of phagocytes. Rev Infect Dis. 1983; 5(5):843–853. [PubMed: 6356269]

35. Matsuzawa A, Saegusa K, Noguchi T, Sadamitsu C, Nishitoh H, Nagai S, Koyasu S, Matsumoto K, Takeda K, Ichijo H. ROS-dependent activation of the TRAF6-ASK1-p38 pathway is selectively required for TLR4-mediated innate immunity. Nat Immunol. 2005; 6(6):587–592. [PubMed: 15864310]

36. Gobert AP, Asim M, Piazuelo MB, Verriere T, Scull BP, de Sablet T, Glumac A, Lewis ND, Correa P, Peek RM Jr, Chaturvedi R, Wilson KT. Disruption of nitric oxide signaling by Helicobacter pylori results in enhanced inflammation by inhibition of heme oxygenase-1. J Immunol. 2011; 187(10):5370–5379. [PubMed: 21987660]

37. Ha H, Kwak HB, Lee SW, Jin HM, Kim HM, Kim HH, Lee ZH. Reactive oxygen species mediate RANK signaling in osteoclasts. Exp Cell Res. 2004; 301(2):119–127. [PubMed: 15530848]

38. Li DZ, Zhang QX, Dong XX, Li HD, Ma X. Treatment with hydrogen molecules prevents RANKL-induced osteoclast differentiation associated with inhibition of ROS formation and inactivation of MAPK, AKT and NF-kappa B pathways in murine RAW264.7 cells. J Bone Miner Metab. 2014; 32(5):494–504. [PubMed: 24196871]

39. Hyeon S, Lee H, Yang Y, Jeong W. Nrf2 deficiency induces oxidative stress and promotes RANKL-induced osteoclast differentiation. Free Radic Biol Med. 2013; 65:789–799. [PubMed: 23954472]

40. Kanzaki H, Shinohara F, Kanako I, Yamaguchi Y, Fukaya S, Miyamoto Y, Wada S, Nakamura Y. Molecular regulatory mechanisms of osteoclastogenesis through cytoprotective enzymes. Redox Biol. 2016; 8:186–191. [PubMed: 26795736]

41. van't Hof RJ, Ralston SH. Cytokine-induced nitric oxide inhibits bone resorption by inducing apoptosis of osteoclast progenitors and suppressing osteoclast activity. J Bone Miner Res. 1997; 12(11):1797–1804. [PubMed: 9383684]

42. Kaisho T, Akira S. Toll-like receptors and their signaling mechanism in innate immunity. Acta Odontol Scand. 2001; 59(3):124–130. [PubMed: 11501880]

43. Brune B, Dehne N, Grossmann N, Jung M, Namgaladze D, Schmid T, von Knethen A, Weigert A. Redox control of inflammation in macrophages. Antioxid Redox Signal. 2013; 19(6):595–637. [PubMed: 23311665]

44. Krisher T, Bar-Shavit Z. Regulation of osteoclastogenesis by integrated signals from toll-like receptors. J Cell Biochem. 2014; 115(12):2146–2154. [PubMed: 25079212]

45. Kajiya M, Giro G, Taubman MA, Han X, Mayer MP, Kawai T. Role of periodontal pathogenic bacteria in RANKL-mediated bone destruction in periodontal disease. J Oral Microbiol. 2010; 2

46. Wang W, Ferguson DJ, Quinn JM, Simpson AH, Athanasou NA. Osteoclasts are capable of particle phagocytosis and bone resorption. J Pathol. 1997; 182(1):92–98. [PubMed: 9227347]
47. Meng B, Yang X, Chen Y, Zhai J, Liang X. Effect of titanium particles on os-teoclast activity in vitro. Mol Med Rep. 2010; 3(6):1065–1069. [PubMed: 21472356]
48. Park OJ, Yang J, Kim J, Yun CH, Han SH. Enterococcus faecalis attenuates the differentiation of macrophages into osteoclasts. J Endod. 2015; 41(5):658–662. [PubMed: 25649294]
49. Yang J, Park OJ, Kim J, Baik JE, Yun CH, Han SH. Lipoteichoic acid of Enterococcus faecalis inhibits the differentiation of macrophages into osteoclasts. J Endod. 2016; 42(4):570–574. [PubMed: 26920932]
50. Takami M, Kim N, Rho J, Choi Y. Stimulation by toll-like receptors inhibits osteoclast differentiation. J Immunol. 2002; 169(3):1516–1523. [PubMed: 12133979]
51. Zou W, Bar-Shavit Z. Dual modulation of osteoclast differentiation by lipo-polysaccharide. J Bone Miner Res. 2002; 17(7):1211–1218. [PubMed: 12096834]
52. Zou W, Schwartz H, Endres S, Hartmann G, Bar-Shavit Z. CpG oligonucleotides: novel regulators of osteoclast differentiation. FASEB J. 2002; 16(3):274–282. [PubMed: 11874977]
53. Ha H, Lee JH, Kim HN, Kwak HB, Kim HM, Lee SE, Rhee JH, Kim HH, Lee ZH. Stimulation by TLR5 modulates osteoclast differentiation through STAT1/IFN-beta. J Immunol. 2008; 180(3): 1382–1389. [PubMed: 18209032]
54. Suzuki H, Mochizuki A, Yoshimura K, Miyamoto Y, Kaneko K, Inoue T, Chikazu D, Takami M, Kamijo R. Bropirimine inhibits osteoclast differentiation through production of interferon-beta. Biochem Biophys Res Commun. 2015; 467(1):146–151. [PubMed: 26399683]
55. Takayanagi H, Kim S, Matsuo K, Suzuki H, Suzuki T, Sato K, Yokochi T, Oda H, Nakamura K, Ida N, Wagner EF, Taniguchi T. RANKL maintains bone homeostasis through c-Fos-dependent induction of interferon-beta. Nature. 2002; 416(6882):744–749. [PubMed: 11961557]
56. Ji JD, Park-Min KH, Shen Z, Fajardo RJ, Goldring SR, McHugh KP, Ivashkiv LB. Inhibition of RANK expression and osteoclastogenesis by TLRs and IFN-gamma in human osteoclast precursors. J Immunol. 2009; 183(11):7223–7233. [PubMed: 19890054]
57. Ishii T, Shimazu Y, Nishiyama I, Kikuta J, Ishii M. The role of sphingosine 1-phosphate in migration of osteoclast precursors; an application of intravital two-photon microscopy. Mol Cells. 2011; 31(5):399–403. [PubMed: 21360199]
58. Movila A, Ishii T, Albassam A, Wisitrasameewong W, Howait M, Yamaguchi T, Ruiz-Torruella M, Bahammam L, Nishimura K, Van Dyke T, Kawai T. Macrophage Migration Inhibitory Factor (MIF) supports homing of osteoclast precursors to peripheral osteolytic lesions. J Bone Miner Res. 2016
59. Nourshargh S, Alon R. Leukocyte migration into inflamed tissues. Immunity. 2014; 41(5):694–707. [PubMed: 25517612]
60. Dempster DW, Lambing CL, Kostenuik PJ, Grauer A. Role of RANK ligand and denosumab, a targeted RANK ligand inhibitor, in bone health and osteoporosis: a review of preclinical and clinical data. Clin Ther. 2012; 34(3):521–536. [PubMed: 22440513]
61. Reyes C, Hitz M, Prieto-Alhambra D, Abrahamsen B. Risks and benefits of bisphosphonate therapies. J Cell Biochem. 2016; 117(1):20–28. [PubMed: 26096687]
62. Epstein MS, Ephros HD, Epstein JB. Review of current literature and implications of RANKL inhibitors for oral health care providers. Oral Surg Oral Med Oral Pathol Oral Radiol. 2013; 116(6):e437–e442. [PubMed: 22901640]

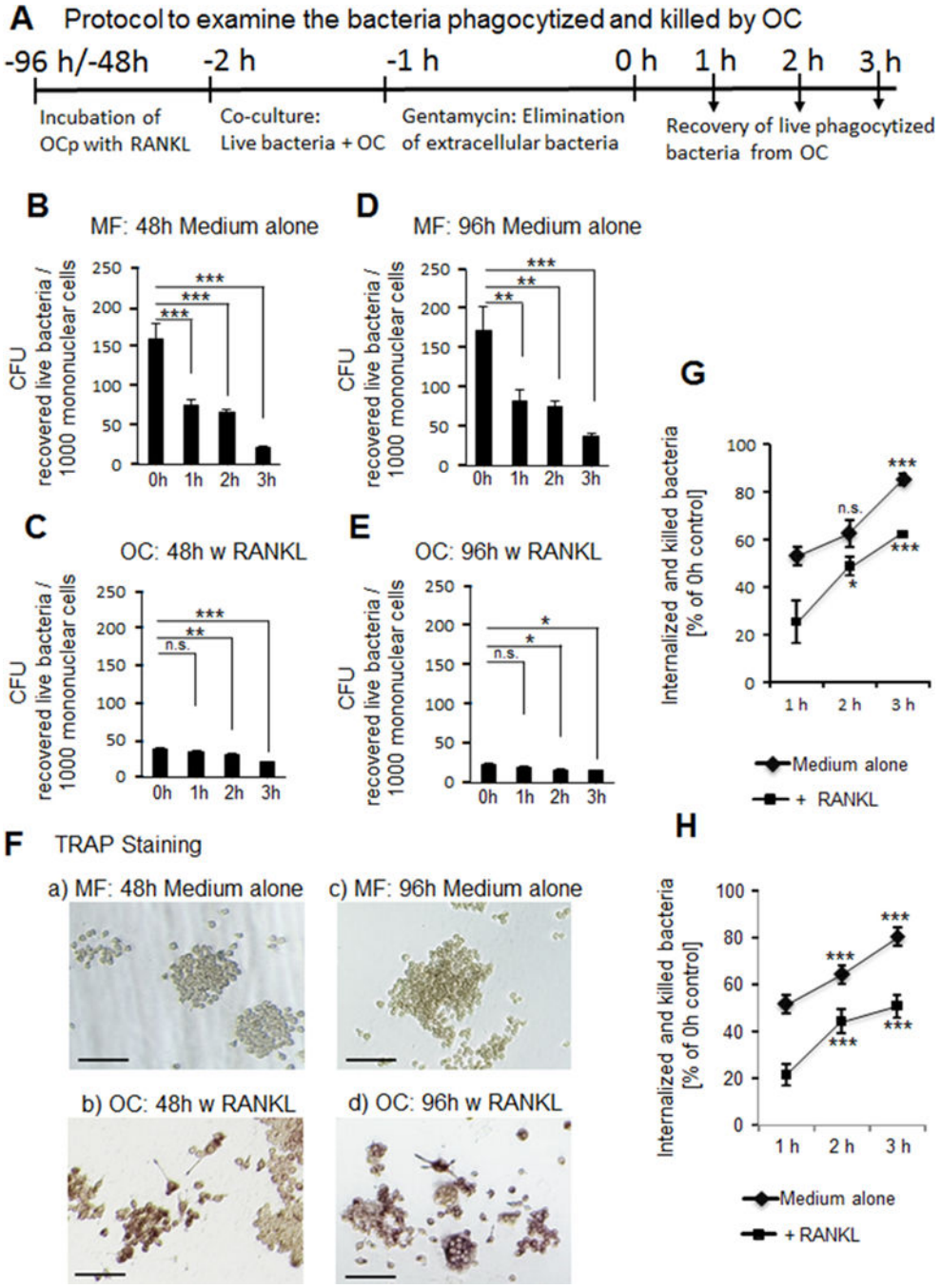

Fig. 1.

Bacteria killing effects by RAW264.7 cells stimulated with/without RANKL. (A) After preincubation of RAW264.7 cells with or without RANKL (50 ng/ml) for 48 or 96 h, *E. coli* entered into the cytoplasm of RAW264.7 cells were evaluated following the protocol described in Materials and Methods. The time line for each specific procedure performed in this experiment is illustrated in [A]. (B–E) The numbers of bacteria which phagocytized by RAW264.7 cells and survived inside of RAW264.7 cells were expressed as a colony forming unit (CFU)/1000 mononuclear cells. RAW264.7 cells were preincubated in medium alone

for 48-h [B] and 96-h [D]. RAW264.7 cells were pre-incubated for 48-h [C] and 96-h [E] with RANKL. (F): TRAP-staining of RAW264.7 cells incubated with or without RANKL for 48-h (a: medium alone, b: with RANKL) and for 96-h (c: medium alone, d: with RANKL) are shown. (G and H) The rates of killed bacteria (%) after each incubation time (1, 2 and 3 h) were calculated based on the comparison with the phagocytized live bacteria counted at base line (0 h). The results of RAW264.7 cells preincubated with or without RANKL for 48-h [G] and for 96-h [H] are shown. Abbreviation in Figure: MF; macrophage (no-stimulated RAW264.7), OC; osteoclasts (Raw264.7 cells stimulated with RANKL). Each column and bar represents mean±SD. *p<0.05, **p<0.01, and ***p<0.001, n.s.–not significant.

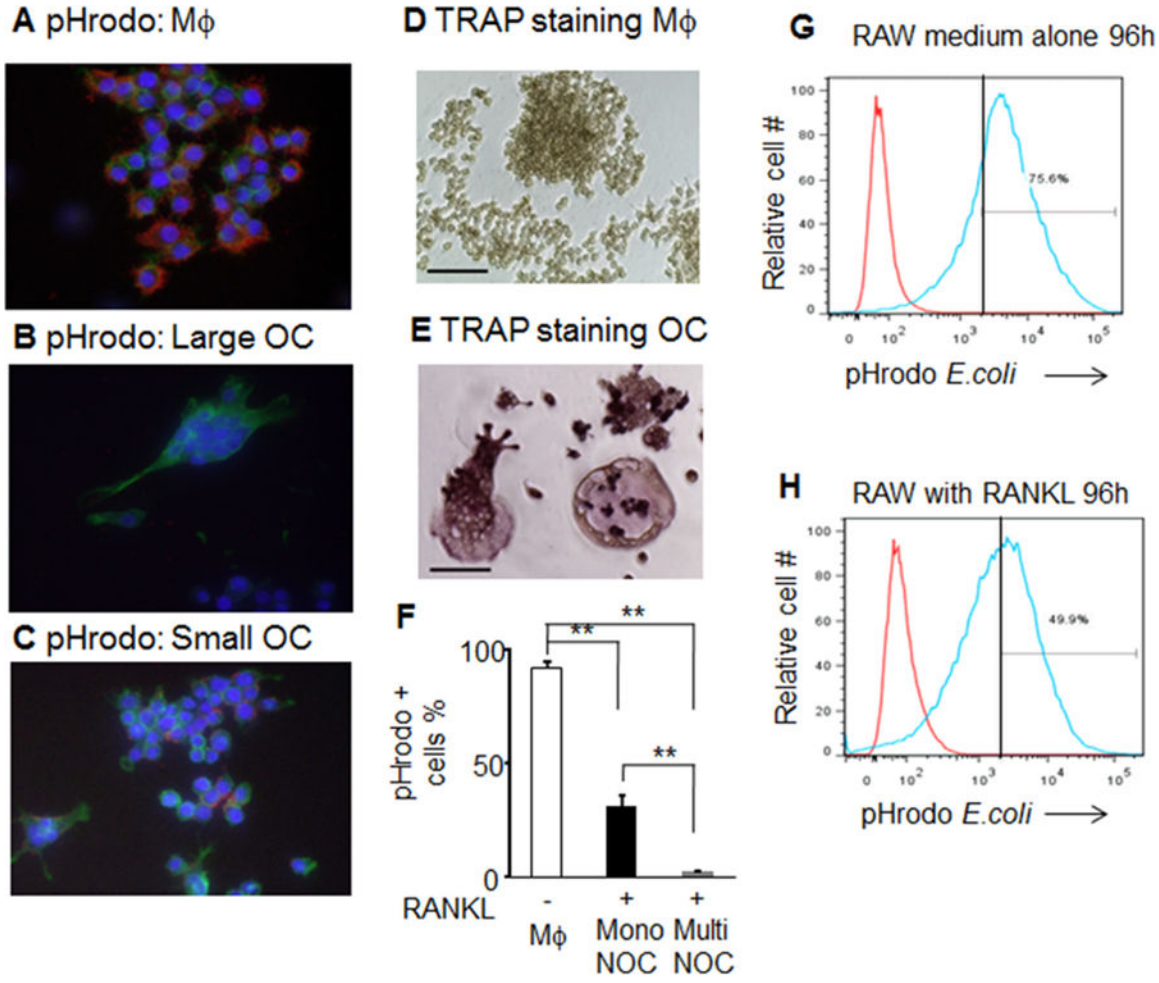

Fig. 2.

The uptake of pHrodo™ Red *E. coli* BioParticles® by RAW 264.7 cells. Fluorescent images of phagocytized *E. coli* BioParticles® in the cytoplasm of RAW264.7 cells that were prestimulated with or without RANKL are shown. (A–C) RAW264.7 cells were preincubated without RANKL [A] or with RANKL [B and C] for 96-h and co-cultured with pHrodo Red *E. coli* BioParticles® for 1 h, then, counter-stained with AlexaFluor 488 conjugated phalloidin (green) and DAPI (blue). Only the phagocytized pHrodo *E. coli* by RAW264.7 cells show the red fluorescent. In the large osteoclast, little or no red fluorescent was detected [B]. In contrast, small osteoclasts showed the red-fluorescent+ pHrodo *E. coli* in the cytoplasm [C]. Images were captured using a fluorescent microscope at 600 × magnification. (D and E): TRAP staining patterns of RAW264.7 cells that were preincubated with or without RANKL for 96 h is shown [D: no RANKL, E: with RANKL]. (F): The % of pHrodo positive RAW264.7 cells was counted from the captured A–C images. ** $p<0.01$ [G and H] In order to quantify the phagocytized pHrodo™ *E. coli* by RAW cells, after 1 h of co-culture with pHrodo *E. coli*, respective RAW264.7 cells, either prestimulated without (G) or with RANKL (H) for 96 h, and then were removed from tissue culture flask using a cell scraper. The resulting single cell suspension of respective RAW cells were subject to FACS

analysis. The cells received pHrodo *E. coli* are indicated in blue and negative controls are in red samples, respectively.

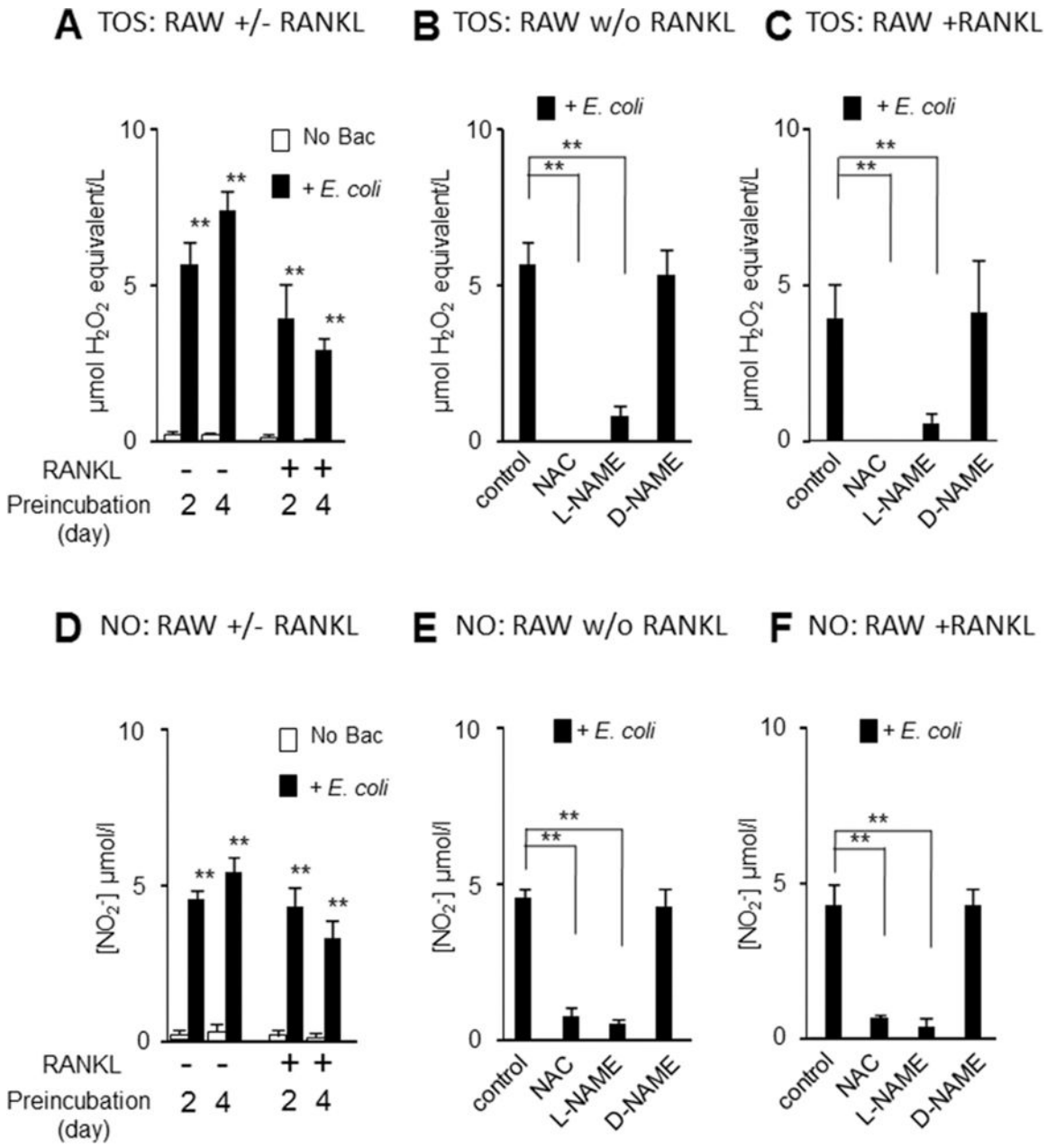

Fig. 3.

Production of ROS and NO from *E. coli*-exposed osteoclasts differentiated from RAW264.7 cells. RAW264.7 cells that were prestimulated with or without RANKL for 48 h were exposed to live *E. coli* for one hour. After elimination of the extracellular bacteria with antibiotics, respective RAW264.7 cells were cultured in fresh medium in the presence or absence of NAC (1 mM), L-NAME (1 mM) or D-NAME (1 mM). After the additional 3 h incubation, the levels of total oxidant status (TOS) and nitric acid (NO) in the culture supernatants were measured. (A): Levels of TOS produced from RAW cells in response to *E. coli* that were prestimulated with/without RANKL for 2 and 4 days (B and C): Effects of NAC and L-NAME on *E.coli*-induced TOS production from RAW264.7 cells that were

prestimulated without RANKL [B] or with RANKL [C]. (D): Levels of NO produced from RAW cells in response to *E. coli* that were prestimulated with/without RANKL for 2 and 4 days (E and F): Effects of NAC and L-NAME on *E.coli*-induced NO production from RAW264.7 cells that were prestimulated without RANKL [E] or with RANKL [F]. $^{**}p<0.01$.

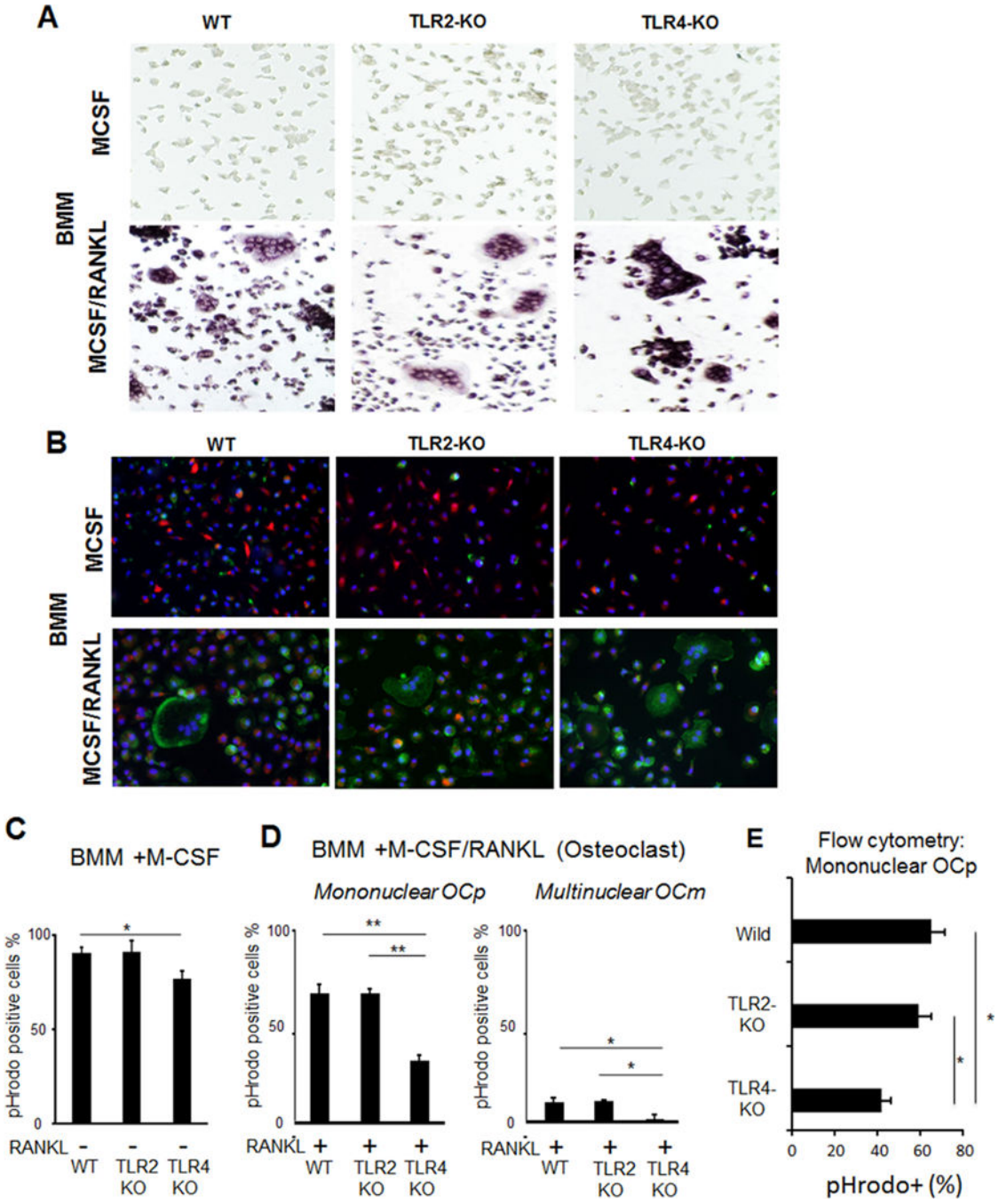

Fig. 4.

The uptake of pHrodo™ Red *E. coli* BioParticles® by osteoclasts differentiated from BMM cells of WT, TLR2-KO and TLR4-KO mice. (A) TRAP staining of WT, TLR2-KO and TLR4-KO bone marrow monocytes (BMM) incubated with M-CSF alone or M-CSF/RANKL for 96 h is shown. (B) BMM cells derived from WT, TLR2-KO and TLR4-KO mice were preincubated without RANKL [A] or with RANKL [B] for 96-h and, then, exposed to pHrodo™ Red *E. coli* for one hour. Subsequently, the cells were counter-stained with AlexaFluor 488 conjugated phalloidin (green) and DAPI (blue). Images of

magnification × 200 are shown. (C) The incidences (%) of pHrodo positive cells were counted from the captured images of BMM cells that were not prestimulated with RANKL. (D) The incidences (%) of pHrodo positive cells were counted from the captured images of BMM cells that were prestimulated with M-CSF/RANKL are shown: (a) pHrodo positive (%) in OCp; (b) pHrodo positive (%) in OCm. (E) The incidences (%) of pHrodo positive cells in mononuclear OCp population were analyzed using a flow cytometer. *$p<0.05$ **$p<0.01$.

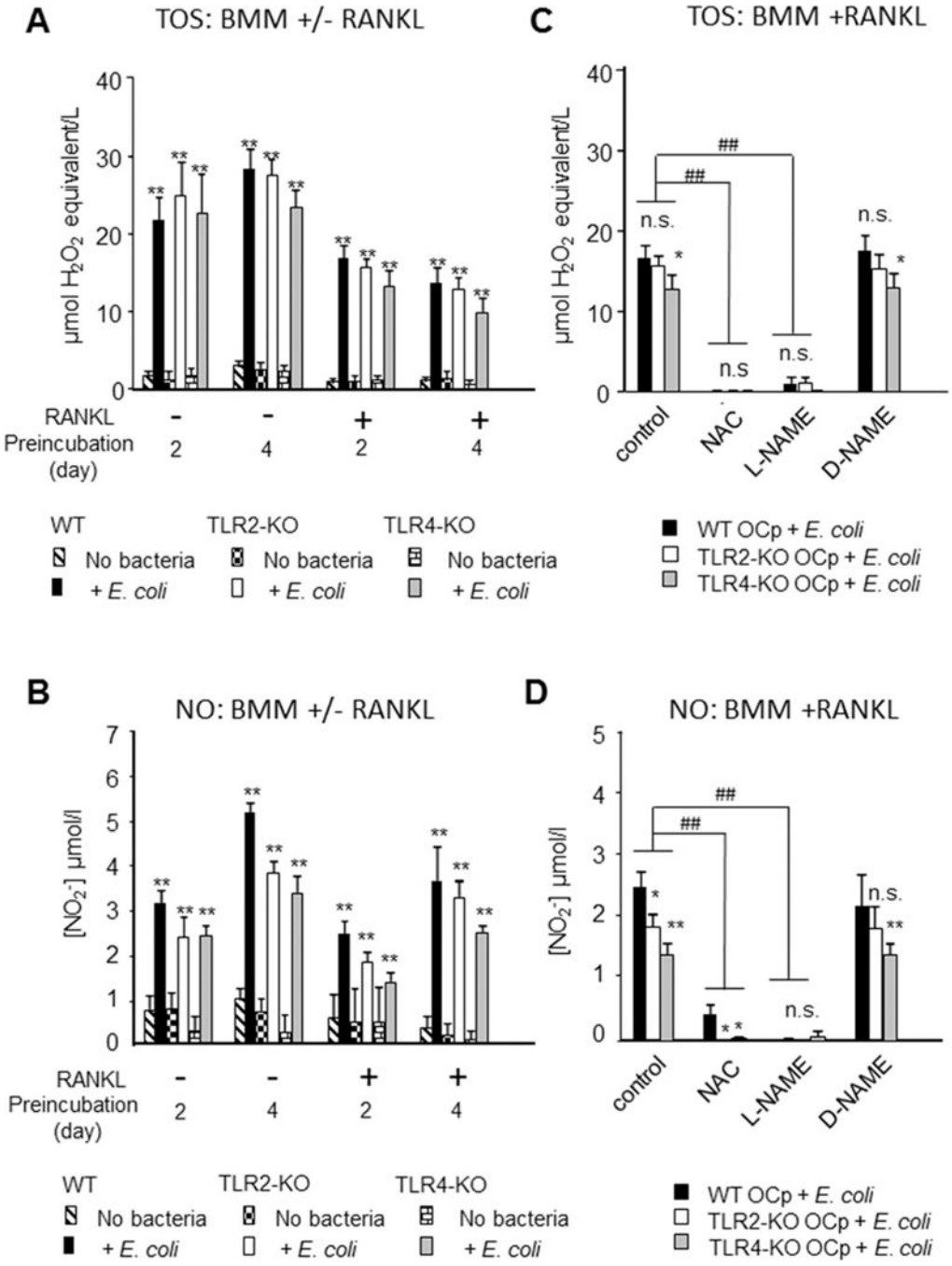

Fig. 5.

Production of ROS and NO from *E. coli*-exposed osteoclasts differentiated from BMM cells of WT, TLR2-KO and TLR4-KO mice. (A and B) Levels of TOS (A) and NO (B) produced from *E. coli*-stimulated BMMs that were preincubated with/without RANKL for 2 and 4 days. (C and D) Effects of NAC and L-NAME on *E. coli*-induced TOS (C) and NO (D) production from BMM that were prestimulated with RANKL in the presence of M-CSF for 48 h. Bone marrow monocytes (BMM) derived from WT, TLR2-KO and TLR4-KO mice were preincubated with or without RANKL in the presence of M-CSF for 48-h and, then,

exposed to live *E. coli* for one hour. After killing the extracellular bacteria with antibiotics, respective BMM cells were cultured in fresh medium in the presence or absence of NAC (1 mM), L-NAME (1 mM) or D-NAME (1 mM). After the additional 3 h incubation, the levels of total oxidant status (TOS) and nitric acid (NO) in the culture supernatants were measured. Each column and bar represents mean±SD from three wells. **$p<0.01$, n.s.–not significant.

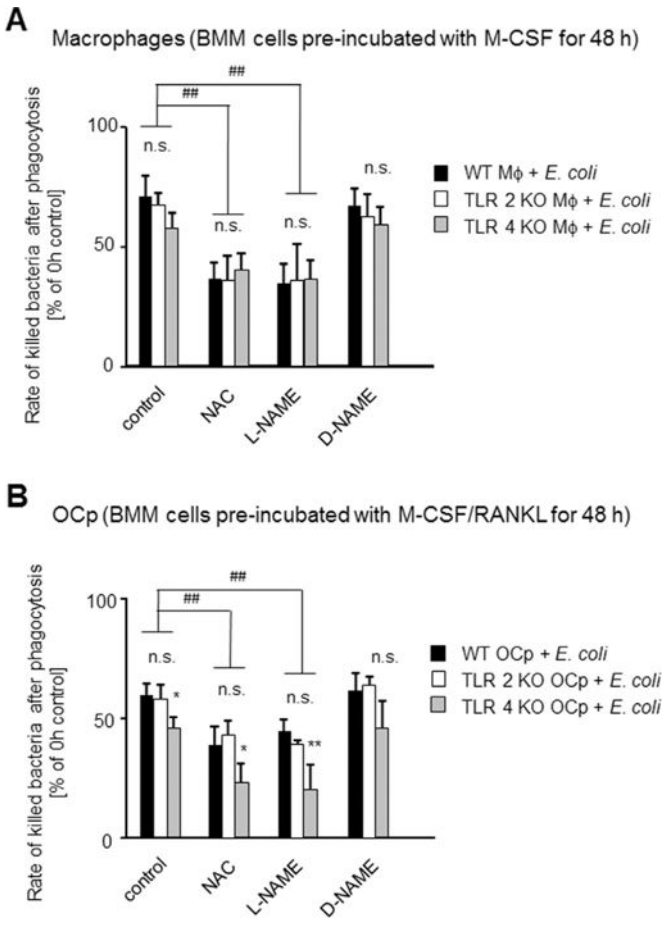

Fig. 6.

Engagement of ROS or NO in the killing of phagocytized bacteria by osteoclast precursors. The killing rates of phagocytized bacteria by control macrophages (A) and OCp (B) that were differentiated from BMM of WT, TLR2-KO and TLR4-KO mice via preincubation with M-CSF alone (A) and M-CSF/RANKL (B) for 48 h are shown. As described in Fig. 5 legend, after elimination of the extracellular bacteria with antibiotics, respective BMM cells were cultured in fresh medium in the presence or absence of NAC (1 mM), L-NAME (1 mM) or D-NAME (1 mM) for 3 h, and CFU of survived *E. coli* in the BMM were counted. The killing rates (%) of phagocytized bacteria after 3 h incubation was calculated in comparison to the phagocytized live bacteria counted at base line (0 h). Each column and bar represents mean±SD of killing rates (%) from three wells. ##$p<0.01$, significantly different between columns indicated by a bracket for the respective strain of mice.

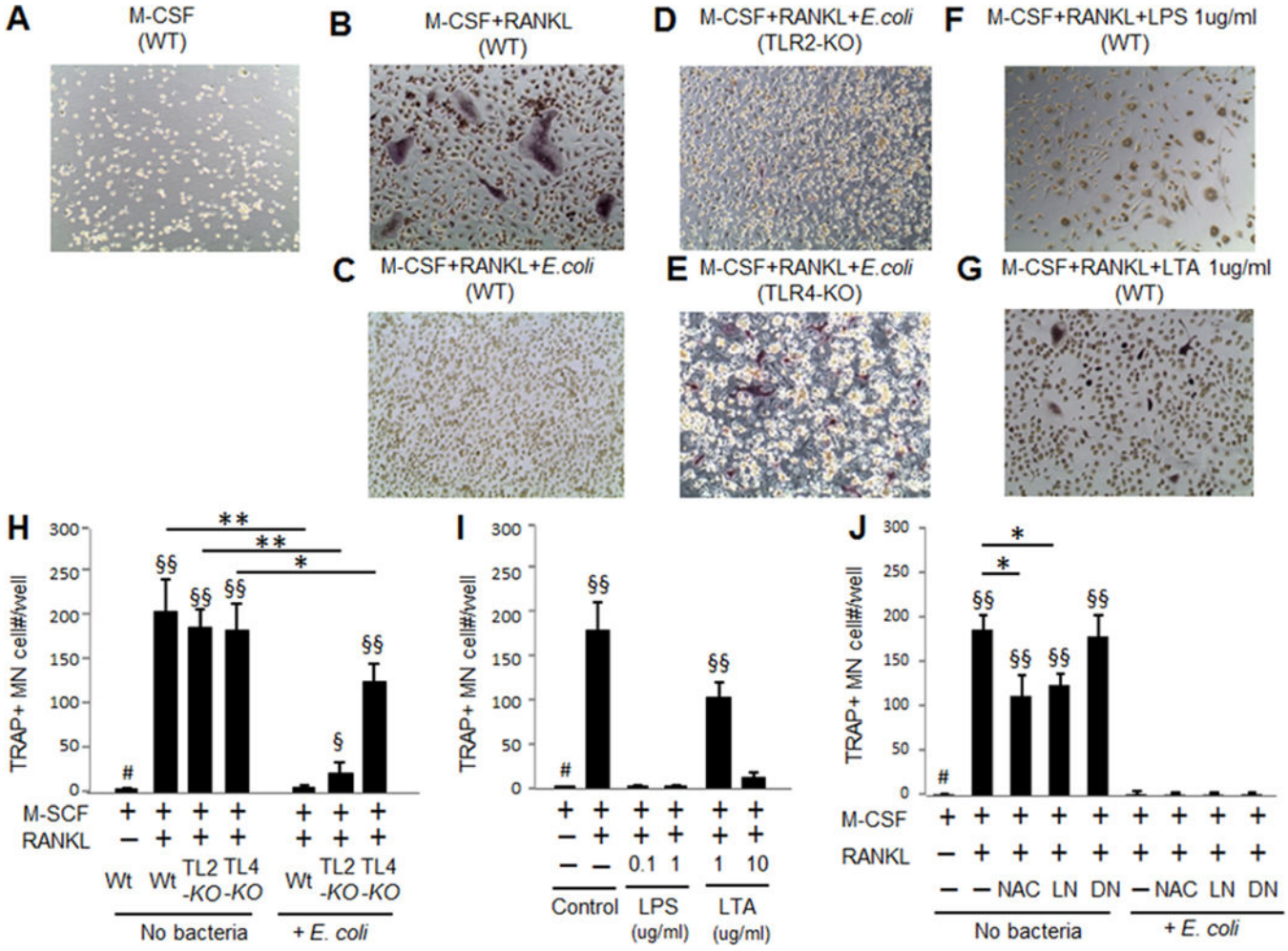

Fig. 7.

Effects of bacteria phagocytosis by OCp on their RANKL-mediated osteoclastogenesis. Osteoclast precursors (OCp) developed in vitro from BMM of WT, TLR2-KO and TLR4-KO mice via prestimulation with M-CSF/RANKL for 2 days were exposed to fixed *E. coli* for 3 h. Subsequently, bacteria-phagocytized OCp were maintained in the culture under continuous M-CSF/RANKL stimulation for additional 5 days. (A-G) Images of TRAP-stained BMM cells after a total of 7 day incubation with M-CSF/RANKL (pre-incubation for 2 days+post-phagocytosis incubation for 5 days) are shown. (H-J) The number of TRAP +multinuclear cells differentiated in the culture was measured. [H] RANKL-induced osteoclastogenesis was compared among three strains of mice, i.e., TLR2-KO, TLR4-KO and WT. [I] Effects of LPS and LTA on the RANKL-induced osteo-clastogenesis from BMM of WT mice were shown. After prestimulation with M-CSF/RANKL for 2 days, WT BMM cells were incubated with or without LPS or LTA for additional 5 days in the presence of M-CSF/RANKL. [J] Effects of NAC, L-NAME (LN) and D-NAME (DN) on the RANKL-induced osteoclastogenesis from BMM of WT mice were shown. Each column and bar represents mean±SD of TRAP+multinuclear cells from three wells. $^{\S}p<0.05$, $^{\S\S}p<0.01$,

significantly different compared to the control M-SCF-stimulation alone (column with #). *p<0.05 **p<0.01, significantly different between the columns indicated by brackets.